

Non-Linear FE-Analysis of a Composite Action Girder with Coiled Spring Pins as Shear Connectors

Simon Stahlin

Civil Engineering, master's level (120 credits)
2019

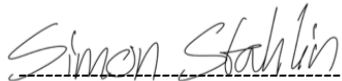
Luleå University of Technology
Department of Civil, Environmental and Natural Resources Engineering

Preface

This thesis is the last part of my Civil Engineering studies at Luleå University of Technology. 5 Years have passed since the beginning and I am very grateful to have met all these people and all the knowledge this time has given me.

I would like to thank my examiner Prof. Peter Collin, who introduced me to this subject. Also, I would like to thank my supervisors Dr. Robert Hällmark and Dr. Rasoul Nilforoush. Robert who helped me with the start and along this thesis and Rasoul who helped me at the end to finish.

Luleå, Maj 2019

A handwritten signature in cursive script that reads "Simon Stahlin". The signature is written in black ink and is positioned above a horizontal dashed line.

Simon Stahlin

Abstract

For bridges to cope with increased requirements such as increased loads, strengthening work can be carried out. In cases where older steel-concrete bridges do not have a composite action, an alternative is to create composite-action to achieve a higher flexural strength. It is introduced by post-installing shear connectors. There are many different alternatives of shear connectors that can be used, hence a number that can be installed from below the bridge to minimize the impact on the traffic. Coiled Spring Pins are of the interference fit type connector and are put in place from below the bridge by first drilling a hole upward through the upper steel flange and then into the concrete slab. Then, the spiral bolt is pushed up into the drilled hole by means of a hydraulic hammer.

Using data from push-out tests and non-linear material models for steel and concrete, a non-linear finite element analysis was created using the commercial finite element software Abaqus. The analysis is based on dimensions and load cases that will mimic a planned full-scale beam test that will be carried out later in 2019. To verify that the material and the model behave in a realistic manner, an analysis was initially performed on a beam without composite-action, and a full-composite action beam with infinitely rigid connectors. These were then compared with hand calculations according to Eurocode.

When the material models were verified, it is seen that the materials steel and concrete work for themselves in the analysis without composite-action and together in the analysis with full composite-action. The data for the spiral bolts is then defined instead of infinitely rigid connectors and new analyzes were performed to see the effect of the coiled spring pins properties.

The results show that a significant increase in the point load in the middle of the beam can take place before failure occurs after installation of this type of shear connector. Already at a low number of connectors and a low shear connection-ratio, a significant increase in the flexural strength is seen in the beam.

By using partial-composite action, with a lower number of spiral bolts, a significant higher flexural strength can be achieved in an economical way.

Keywords: composite bridge; composite action; shear connector; coiled spring pins; finite element modeling

Sammanfattning

När kraven på att broar ska klara av ökade laster, kan förstärkningsarbeten utföras. I de fall där äldre stål-betongbroar saknar samverkansseffekt, är det ett alternativ att införa samverkan för att uppnå en högre böj-hållfastighet. Det införs genom att man installerar skjuvförbindare i efterhand. Det finns många olika alternativ av skjuvförbindare som kan användas, därav ett antal som går att installera underifrån bron för att minimera påverkan på trafiken. Spiralbultar (Coiled Spring Pins) är av typen presspassnings-förbindare och sätts på plats underifrån bron genom att det först borrar ett hål uppåt genom övre stålflänsen och sedan upp i betongplattan. Därefter pressas spiralbulten upp i det borrarade hålet med hjälp av en hydraulisk hammare.

Med hjälp av data ifrån push-out-tester samt icke-linjära material modeller för stål och betong, skapades en icke-linjär analys i det finita element metods programmet Abaqus. Analysen är uppbyggd med dimensioner och lastfall som ska efterlikna ett planerat full-skaligt balktest som kommer utföras under 2019. För att verifiera att materialet och modellen beter sig realistiskt, utförs en analys på en balk utan samverkan, samt en full-samverkans balk med oändligt styva förbindare. Dessa jämförs sedan med handberäkningar enligt Eurokod.

När materialmodellerna var verifierade sågs det att materialen stål och betong arbetar för sig själva i analysen utan samverkan och tillsammans i analysen med full-samverkan. Data för spiralbultarna lades sedan in istället för oändligt styva förbindare och nya analyser utförs för att se påverkan av spiralbultarnas egenskaper.

Resultaten visade att en betydande ökning av punklasten i mitten av balken kan ske innan brott uppstår vid installation i efterhand av denna typen skjuvförbindare. Redan vid ett lågt antal förbindare och ett lågt skjuv-förhållande ses en betydande ökning av böj-hållfastheten i balken.

Genom att använda delvis-samverkan med ett lägre antal spiralbultar kan man på ett ekonomiskt sätt uppnå en betydligt högre böj-hållfasthet.

Nyckelord: samverkansbro; samverkan; skjuvförbindare; spiralbult; finita element modellering

Nomenclature

Abbreviations

CDP	Concrete Damage Plasticity
CSP	Coiled Spring Pin
FEA	Finite Element Analysis
FEM	Finite Element Method

Geometry

$A_{eff,concrete}$	Effective concrete area
$A_{concrete}$	Area of concrete cross-section
A_{steel}	Area of steel cross-section
c-c	Center to Center
CG	Center of gravity
h_c	Height of concrete slab
h_w	Height of web
t_{lf}	Thickness of bottom flange
t_{uf}	Thickness of top flange
t_w	Thickness of web
w_c	Width of concrete slab
w_{lf}	Width of bottom flange
w_{uf}	Width of top flange

Material

β	Slope factor used to calculate compressive strength
b_c	Parameter used to calculate d_c
b_t	Parameter used to calculate d_t
d_c	Damage parameter in compression
d_t	Damage parameter in tension
E	Modulus of elasticity
E_0	Initial modulus of elasticity
E_a	Steels modulus of elasticity
E_{it}	Initial concrete modulus of elasticity
E_{cm}	Concretes mean modulus of elasticity

E_{ra}	Reinforcement elastic modulus
ε	Strain
ε_0	The strain where f'_c occur
ε_{0c}^{el}	Initial elastic strain in compression
ε_c	Compressive strain
ε_c^{in}	In-elastic strain in compression
ε_c^{pl}	Plastic compressive strain
ε_{nom}	Nominal strain
ε_t	Tension strain
ε_t^{in}	In-elastic strain in tension
ε_{true}	True strain
$\varepsilon_{true}^{plastic}$	True plastic strain
ε_t^{pl}	Plastic tension strain
ε_{sh}	Strain at strain hardening
ε_u	Strain when steel reaches its ultimate strength
ε_y	Strain when steel starts to yield
$f_{cu} = f'_c$	Ultimate compressive strength of concrete
f_{ry}	Reinforcement yielding limit
f_{tcm}	Tensile strength of concrete
f_y	Yielding strength of steel
n	factor used to calculate compressive strength
σ_{nom}	Nominal stress
σ_{t0}	Ultimate tensile stress
σ_{true}	True stress

Table of Contents

Preface.....	i
Abstract	ii
Sammanfattning.....	iii
Nomenclature.....	iv
1 Introduction.....	1
1.1 Background and Research Motivation	1
1.2 Aim and Scope	1
1.3 Limitations	1
1.4 Earlier Research	2
1.5 Method	2
1.6 Outline of Thesis.....	3
2 Composite Bridges.....	4
2.1 None- Composite Action	4
2.2 Full- Composite Action	4
2.3 Partial- Composite Action.....	5
3 Achieving Composite Action.....	6
3.1 Headed studs.....	6
3.2 Post-installed Shear Connectors	6
3.2.1 Coiled Spring Pin.....	7
4 FE Modelling.....	9
4.1 Numerical models.....	9
4.2 Geometry and Material Data	9
4.2.1 Steel girder and shear connector	10
4.2.2 Concrete slab	11
4.2.3 Rebars.....	11
4.3 Boundary Conditions and Loading	12
4.4 FE Discretization	12
4.5 Material Model.....	13
4.5.1 Steel.....	13
4.5.2 Concrete	15
4.6 Shear Connector	19
4.7 Implementation of Analyses.....	19
5 Verification of FE Models	21
5.1 FE verification examples.....	21
5.2 Hand Calculations	21

5.3	Comparison of FEM and Hand Calculations	22
5.3.1	Non- Composite Action	22
5.3.2	Full- Composite Action	23
6	Numerical Studies	24
6.1	With and Without Full-Composite Action	24
6.2	Case 1 (CSP's concentrated near the supports)	25
6.3	Case 2 (evenly distributed CSPs)	25
6.4	Different number of CSP's per meter.....	26
6.5	Slip and Uplift	28
6.5.1	Vertical Displacement.....	29
7	Conclusions.....	30
7.1	CSP	30
7.2	Recommendations to the Laboratory Beam Test	30
7.3	Further Research	30
8	References.....	31
	Appendix A – Hand Calculations.....	33
	Appendix B – Parameters used in the concrete model.....	36

1 Introduction

1.1 Background and Research Motivation

There are a number of old non-composite steel-concrete bridges under service in Sweden which needs strengthening due to today's demand for higher traffic loads. One alternative for strengthening is to develop a composite action between the concrete deck and the steel girder so that both elements work as a composite element. The shear and flexural bending capacity of a non-composite bridge increases significantly by achieving the composite action between the steel girder and concrete deck. In fact, the load bearing capacity in a composite steel-concrete cross-section increases by utilizing the high tensile strength of steel girder (in the tensile zone) and the compressive strength of concrete deck (in the compressive zone).

The composite action can be achieved by post-installing shear connectors between the top flange of the steel girder and the concrete slab. Various post-installed shear connectors are available for this reason, see examples in figure 3.2 in chapter 3.

This research is about finding out how much the flexural strength is increasing with Coiled Spring Pins (CSP's) installed. CSP is a type of shear connector that has the advantage that it can be installed from below the bridge and it is therefore not necessary to close all the traffic over the bridge. With a large increment in the flexural strength and not so much disturbance of the traffic, installing the CSP could be a very effective method to strengthen old steel-concrete bridges without any composite action. By using numerical analyses to find the increments of installing CSP's, realistic insight can be found and afterwards compared with the planned laboratory test.

1.2 Aim and Scope

The overall aim of this study was to assess the structural behavior of composite steel-concrete beams, which have the Coiled Spring Pins (CSP's) as shear connectors, in comparison with non-composite steel-concrete beams. As physical tests are usually expensive and require lots of preparations, the behavior of non-composite and composite beams was numerically analyzed by means of the Finite Element Method (FEM) using the commercial FE-software Abaqus. The numerical analysis helped to evaluate the influence of the amount and position of CSP's along the beam on the structural behavior of composite beams. In particular, this study aimed to answer the following questions:

- (a) What is the structural behavior of non-composite beams that are strengthened with post-installed CSP's?
- (b) Whether a partial composite action is effective as much as a full composite action?
- (c) Whether the local placement of CSP's close to the beam supports is as effective as their evenly distributed placement along the beam?
- (d) What is the influence of rigid and non-linear shear connectors?

The present study provides a better understanding of the performance of CSP's for the strengthening of non-composite bridges. It should be noted that, a full-scale experimental study is currently planning to be carried out at the Luleå University of Technology. The present numerical study provides a better prediction of the failure load and failure mechanism of the testing composite beams for the ongoing experimental study.

1.3 Limitations

Like all numerical studies, the current study was subjected to several limitations. In this study, all FE analyses are performed with boundary conditions of a simply supported girder and a point load in the middle. The length of the girder and position of supports were identical in all FE analyses.

In the FE analyses, the welds on the steel girder are not modeled and it is assumed that the top and bottom flanges are rigidly connected to the web. In addition, the friction at the concrete and steel interface is taken into consideration for the FE analyses, albeit this is neglected in the hand calculations.

Furthermore, the moment of inertia of the concrete slab is considered in the FE analyses, while this is omitted in the hand calculations.

In FE analyses, the failure is characterized once the steel beam reaches its yielding strength at the lower flange. The failure is also considered to occur when the stresses at the top surface of the concrete slab exceed the concrete compressive strength or if the stresses at the bottom surface of the concrete slab exceed the concrete tensile strength.

1.4 Earlier Research

Earlier research on CSP's has mainly been performed by Dr. Hällmark and Prof. Collin at the Luleå University of Technology. The research has been presented in (Hällmark, 2018a). Also, (Olsson, 2017) have presented related information about shear connectors and case studies where they have been used. In the thesis, a study of a Swedish bridge called the Pitsund Bridge has been performed, which has been strengthening with Coiled Spring Pins.

There have been some similar studies to this thesis where FE-analysis has been performed to test different shear connectors. (Kwon G. , 2008) presented experimental and numerical studies on three different shear connectors. Kwon used the FE-program Abaqus in his numerical studies. He implemented shell-elements for both the concrete slab and the steel beam, whereas he used a so-called connector "Cartesian" for the shear studs.

The behavior of composite beams with various types of post-installed shear connectors has been numerically studied by other researchers (see for example, (Tahmasebinia, et al. 2012; Thevendran, et al.1999; El-Lobody & Lam, 2003; Prakash, et al. 2011). In all these studies, the composite beams were simulated in Abaqus and the concrete slab and the steel beam were modelled with solid-elements and the reinforcement with beam-elements. The shear connectors were modeled as spring elements or as solid elements.

1.5 Method

In this thesis, a Finite Element (FE) numerical study was carried out to study the structural behavior of composite steel-concrete beams, which have the Coiled Spring Pins (CSPs) as shear connectors, in comparison with non-composite steel-concrete beams. A simply-supported steel-concrete beam with the free span of 6600 mm was simulated and analyzed using the FE software Abaqus. Three different cases were studied: (a) a non-composite beam with no shear connector, (b) a composite beam with a partial composite action, and (c) a composite beam with a full composite action. In all cases, the geometry of the beams and the support and loading conditions were identical. The beams were locally loaded at the midspan until failure. The failure is considered to happen when the bottom steel flange reaches its yielding strength or if the concrete slab reaches its ultimate tensile or compressive strength.

Therefore, non-linear material models were used for concrete and steel to simulate the behavior of the materials more accurately. The numerical modeling and analysis were verified by comparing the results of analysis (for the non-composite beam) with the predictions according to (EN 1994-2, 2005).

To realistically simulate the behavior of shear connectors, the CSPs are modeled using the non-linear load-displacement data obtained from a previous push-out test on CSPs at the Luleå University of Technology (for details of the experiments see Hällmark, 2018a).

The results of the numerical study are presented in terms of distribution of longitudinal stresses along the beams' cross-section, failure load and failure mode.

1.6 Outline of Thesis

Chapter one, presents the research background, aims, scope, limitations, method, earlier work and the outline of the study.

Chapter two, describes the effect of achieving a composite action in bridges in non-composite bridges.

Chapter three, presents different solution to create a composite action by using post-installed shear connectors.

Chapter four, describes how the FE-modeling's were carried out and what properties were used.

Chapter five, presents a verification of the FE-model, as it is compared to calculations by (EN 1994-2, 2005).

Chapter six, presents the results of the performed FE-analysis and discussions about the results.

Chapter seven, presents the conclusions drawn from the results of FE-analyses and some recommendations for the ongoing full-scale beam tests. Also, some further research ideas are presented in this chapter.

Appendix A presents the hand calculations, which are used to verify the FE-model.

Appendix B shows the values used for defining and modeling the concrete material model used in Abaqus.

Appendix C illustrates different types of post-installed shear connectors.

2 Composite Bridges

A composite bridge is a type of bridge built with the two materials steel and concrete working together as one structural component. The concrete slab is connected to the steel girder with shear connectors which transfer the horizontal shear force at the interface between the two components (Kwon, et al., 2007).

Composite action between the steel beam and concrete slab in a bridge is today a standard choice when using the two materials together. But it has not always been like this in the past. Until the 1980's, there were still composite bridges in Sweden built without any composite action (Hällmark, 2018a). In bridges where there is no composite action, it can be created afterward. It is achieved by post-installed shear connectors which are installed between the upper flange of the steel beam and the concrete slab. Different kinds of shear connectors and methods of achieving a composite action are explained in chapter 3.3.

2.1 None- Composite Action

A bridge with non- composite action has the steel and the concrete work like individual components (see an illustration of a non-composite beam and a composite beam in figure 2.1. As illustrated in figure 2.1a, a slip will occur at the interface between the two components since the two components are not connected to each other.

The concrete slab and the steel beam have their own center of gravity in the middle of each element, where the neutral axis of each element is located. An exemplified description of the distribution of strains along the height of the cross-section with non- composite action is shown in figure 2.2a.

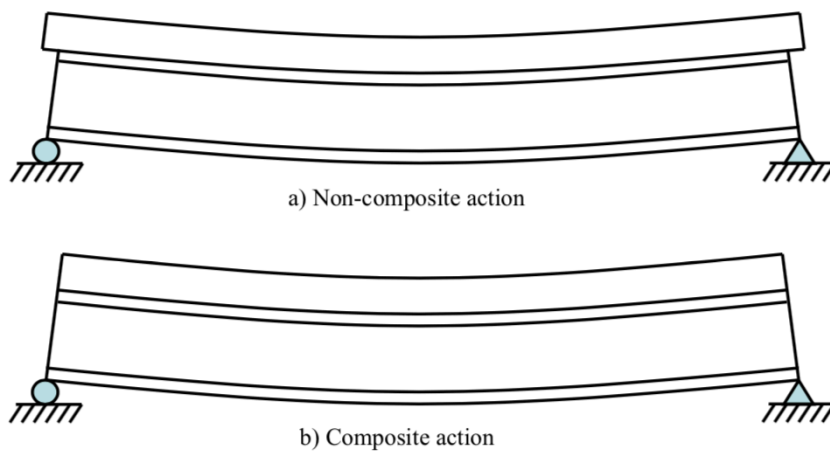


Figure 2.1 Illustration of a) non- composite action and b) composite action, redrawn from (Kwon G. , 2008)

2.2 Full- Composite Action

It is known that steel material is strong in tension while concrete material is considerably weak under tension. To receive a higher flexural and shear capacity of a section made of the two materials, a composite action is often created between the two materials. To achieve this, some sort of shear connector is installed at the interface between the two components. When the two materials are connected together, they will start working as one component. This will let the two materials have one common neutral axis, which will now be located closer to the top steel flange. The strain distribution is now linear throughout both materials (see an illustration of strain distributions for a composite section in figure 2.2b).

To create a full composite action between the components, the shear connector is not allowed to be the part that goes to failure. Instead the steel girder or the concrete slab must be the component that fails. (Olsson, 2017)

2.3 Partial- Composite Action

When the flexural strengths of the girder are decided by the shear connectors strength and not the concrete slabs plastic limit state, there is a partial composite action in the girder. (Olsson, 2017)

When a structure is designed with a partial composite action there will be a slip between the surface of the steel and concrete. This slip makes the strain curve a bit different as can be seen in figure 2.2c.

According to (Kwon G. , 2008) the shear connection ratio can be defined by the number of used shear connectors divided by the total number necessary to create full composite action. A bridge with no shear connectors has therefore a shear connection ratio of zero and works as a non- composite action bridge.

All steel-concrete bridges have some degree of partial composite action. A steel-concrete structure without any kind of shear connector will still be affected by forces creating some composite action, for an example is friction created in the surfaces between the two materials. And even with enough shear connectors to occur full- composite action, there will still be some slip due to displacement in the shear connectors and crushing in the concrete, which will result in a lower degree of composite action. (Hällmark, 2018a)

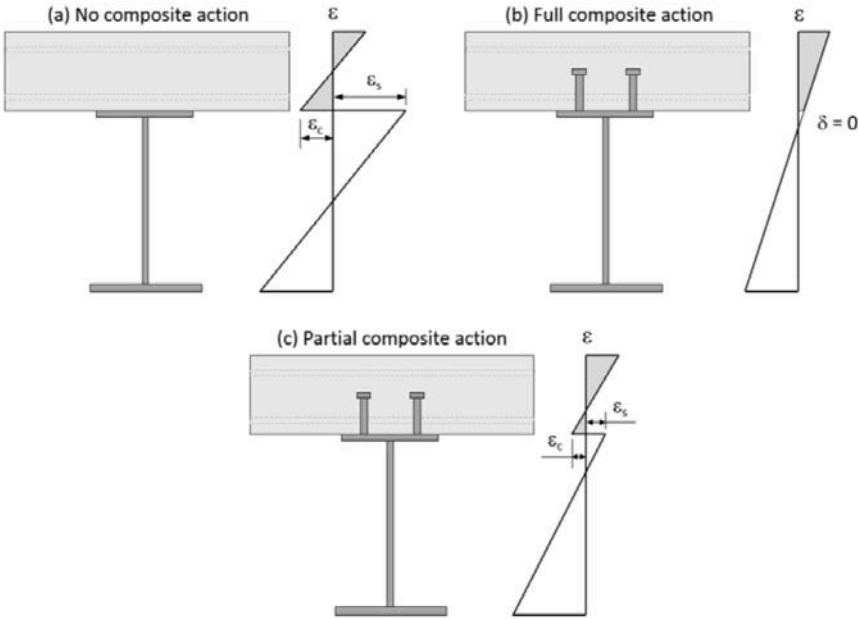


Figure 2.2 Illustration of vertical strain in a steel-concrete structure with a) No composite action b) Full composite action and c) partial composite action, redrawn from (Hällmark, 2018a)

3 Achieving Composite Action

Composite action is created as explained in chapter 2 by connecting the concrete slab to the steel girder with shear connectors. Either the shear connectors are installed when the bridge is being built or they are post-installed. Different methods and shear connectors are described below in sections 3.1 and 3.2.

By creating composite action for a non-composite steel-concrete section, the flexural and shear capacity of the cross-section increases significantly. An example of the theoretical differences between the stresses in the bottom and top steel flanges of non-composite bridge with a composite bridge can be found in chapter 5.2.

In construction of new bridges, shear connectors are often pre-installed in the building process. There are several advantages of pre-installed shear connectors compared to post-installed ones. The pre-installed connectors (which are also known as cast-in place connectors) are more time-effective and their installation can be performed offsite under a controlled environment.

In general, when the shear connectors are exposed to high stresses, they may have a ductile or brittle behavior. The difference is mainly on how the connector deforms when the load capacity is being reached. A ductile connector maintains its ultimate load capacity over a displacement while a brittle connector loses its capacity quickly after reaching the peak load. (Olsson, 2017)

3.1 Headed studs

The headed stud, shown in figure 3.1 is the most commonly used shear connector in new steel-concrete bridge structures. After the stud is welded onto the steel flange the concrete is cast on top of the girder.

Headed studs are often pre-installed during the construction of new composite bridges. They can also be used as post-installed connectors for developing a composite action in existing non-composite bridges. However, their post-installation procedure requires a lot of efforts and preparations. In addition, the bridge needs to be partly or entirely close for such an operation. In post-installation cases, first, the concrete, waterproof layer and pavement layer should be removed and then the studs need to be welded through a lot of reinforcement bars which often makes the access to the top steel girder very limited.

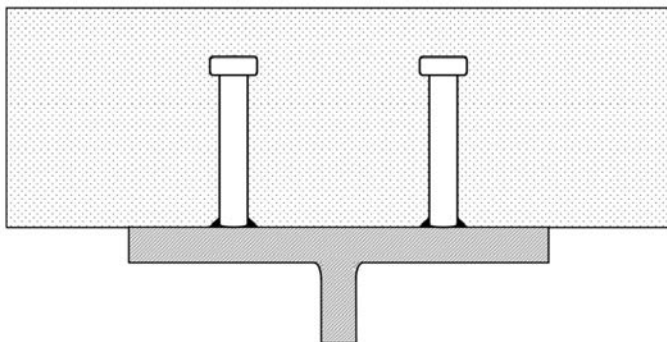


Figure 3.1 Welded stud, redrawn from (Kwon, et al., 2007)

3.2 Post-installed Shear Connectors

There are different types of post-installed shear connectors used for developing composite action in a non-composite bridge. They can be installed from above the concrete deck or below the upper steel flange. Examples of the post-installed shear connectors are shown in figure 3.2.

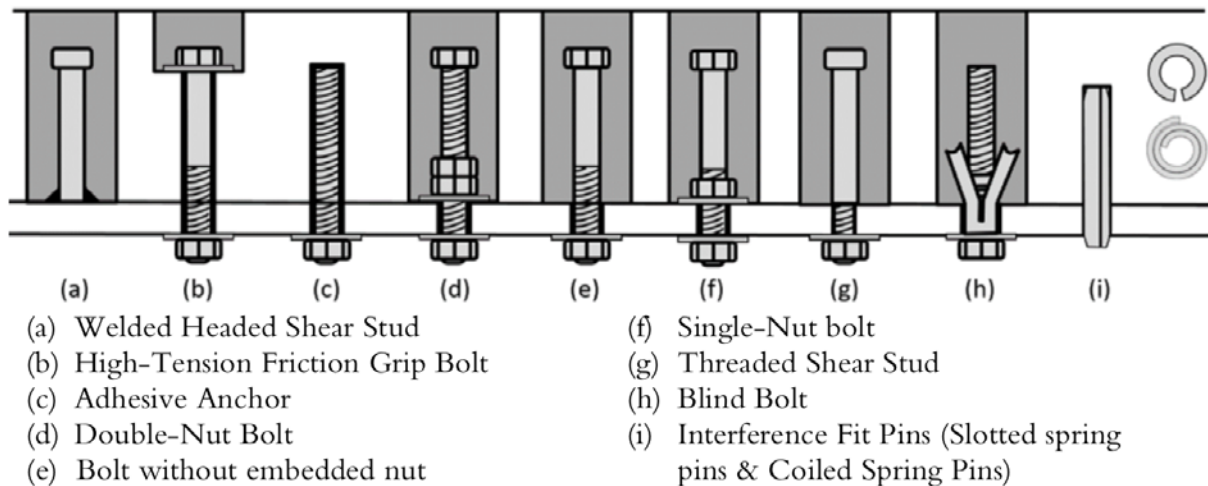


Figure 3.2 Illustration of different post-installed shear connectors, withdrawn from (Hällmark, 2018a).

The post-installed shear connectors can transfer shear forces through three different load-transfer mechanisms. The most commonly used connector utilizes bearing/mechanical interlock load-transfer mechanism, which is used for headed studs. The headed stud transfers the shear force by bearing the concrete slab on the top of the steel flange. Some connectors utilize a friction mechanism for transferring the horizontal shear force (e.g. interference pin). A normal compressive force is created at the surface between the steel connector and concrete when tension in the connector is achieved. This gives a high stiffness and is an ideal mechanism for fatigue problems. Another load-transfer mechanism is adhesion, which can be created by applying a structural adhesive between the steel beam and concrete slab. (Kwon, et al., 2007). In addition, a structural adhesive can be used for bonding post-installed connectors inside pre-drilled holes in a concrete deck.

If the bridge has a planned maintenance of the concrete deck, it is a good opportunity to install any kind of a post-installed shear connector, especially a connector that is installed from above. When there is no planned maintenance another solution like installation from below may be more interesting due to the limited disruption of the traffic. There are several different shear connectors that are possible to install from below. An example of them is the Coiled Spring Pin (CSP), which is focused on in this thesis.

3.2.1 Coiled Spring Pin

The post-installed shear connector, which is being analyzed by a FE-model later in this thesis, is the coiled spring pin (see figure 3.3). A CSP connector is created from a steel plate that is rolled approximately 2,25 times around the central axis of the pin. This type of connector is especially used in industries, where it can have dimensions from less than 1mm to the heavy-duty type of 20mm used in this thesis. (Hällmark, 2018a)



Figure 3.3 Coiled spring pin, redrawn from (Hällmark, Collin, & Hicks, 2018b)

The coiled spring pins have the ability to be post-installed without interrupting the traffic on the bridge. It can be installed from below the bridge with only a small part of a lane closed. They are installed in holes drilled from below the top steel flange into the concrete slab. A hydraulic hammer jack is utilized for inserting the CSPs into the holes, as the size (i.e. diameter) of the CSP is often larger than the drilled hole. The installation procedure as can be seen in figure 3.4. The CSP's create an interference frictional fit into the holes, which means that they do not need any welding, bolts or adhesive to stay in place. In fact, the interference fit is created by a radial spring force that is generated in the pin after installation.

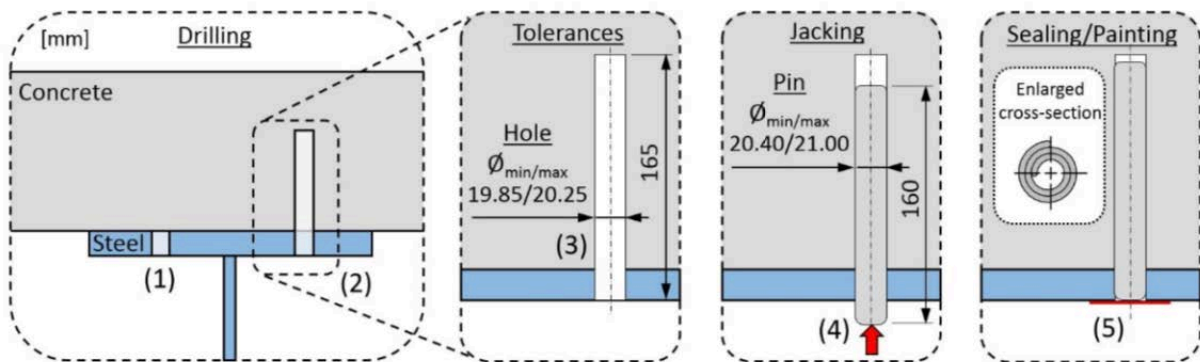


Figure 3.4 Installation of a CSP step by step , redrawn from (Hällmark, 2018a)

4 FE Modelling

This FEA is solved by the static method Rik's, as well as the static general method. Rik's method continues calculating after the maximal load is reached while the general method stops as the defined load is reached. Simpsons rule are used to calculate all material sections and 3 integrations points have been used.

Abaqus has no pre-defined SI-system; however, the user must define the input parameters with consistent units. The SI-units presented in table 4.1 were applied for all analyses.

Table 4.1 SI-units used in Abaqus

Quantity	SI (mm)
Length	mm
Force	N
Mass	ton (1000kg)
Time	s
Stress	MPa (N/mm^2)
Energy	mJ
Density	ton/mm^3

The in-data necessary in Abaqus is not engineering constants such as nominal stress and nominal strain. The calculated stresses and strains need to be converted to true stress and true strain. In the cases plastic strain is being uses, the nominal strain must be converted to logarithmic plastic strain. This is being done to describe the current state of the material with respect to previously performed states and not respect to the un-deformed ones that nominal stress and strain does. The nominal stress and strain values can be converted to "true" values, either by Abaqus convertor function or by using Eq. (4.1), (4.2) and (4.3) as presented below:

$$\sigma_{true} = \sigma_{nom} * (1 + \varepsilon_{nom}) \quad (4.1)$$

$$\varepsilon_{true} = \ln(1 + \varepsilon_{nom}) \quad (4.2)$$

$$\varepsilon_{true}^{plastic} = \ln(1 + \varepsilon_{nom}) - \frac{\sigma_{true}}{E_0} \quad (4.3)$$

4.1 Numerical models

As mentioned before, a Finite Element (FE) numerical study is carried out to study the structural behavior of composite steel-concrete beams, which have the Coiled Spring Pins (CSPs) as shear connectors, in comparison with non-composite steel-concrete beams. A simply-supported steel-concrete beam with the free span of 6600 mm is simulated and analyzed using the FE software Abaqus. Three different cases were studied: (a) a non-composite beam with no shear connector, (b) a composite beam with a partial composite action, and (c) a composite beam with a full composite action. In all cases, the geometry of the beams and the support and loading conditions are identical. The beams are locally loaded at the midspan until failure.

4.2 Geometry and Material Data

Figure 4.1 describes the geometry of the steel girder and concrete slab. The position of applied load and the span length as well the edge distance from the support are also shown in this figure. These dimensions are chosen to mimic a real full-scale beam test.



Figure 4.1 Illustration of dimensions of the girder

In table 4.2, the quality of materials are described. From these qualities, other necessary parameters are calculated to describe the material properties.

Table 4.2 Material qualities

Construction part	Material quality
Steel girder	S355
Steel plates	S355
Coiled Spring Pin	S355
Concrete slab	C32/40
Reinforcement bars	B500

4.2.1 Steel girder and shear connector

Figure 4.2 shows the dimensions of the steel girder and shear connectors that are modelled in Abaqus. The steel girder has a web of dimensions L700xH250xT12 mm, top and bottom flanges of dimension L7000xW250xT30 mm, and six steel plates of dimensions H250xW110xT15 mm as the stiffening plates (three in each side). The shear connectors have a nominal diameter of 20 mm and a height of 125 mm.

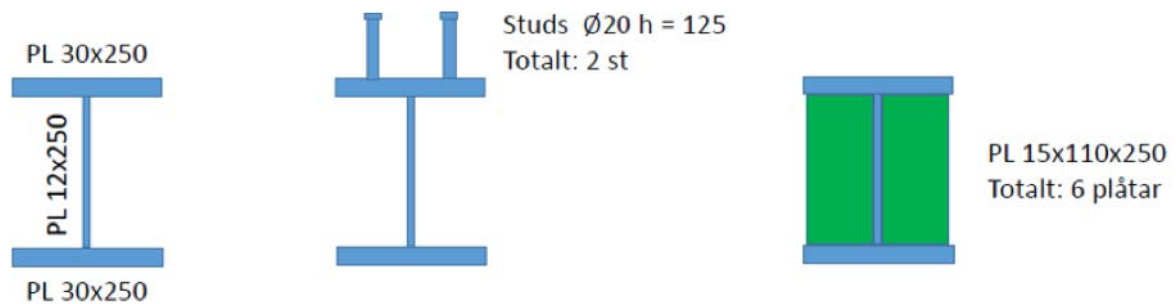


Figure 4.2 Cross-section dimensions of the steel beam

Table 4.3 presents the properties of the structural steel quality S355 which are retrieved from (EN 1993-1-1, 2005). The steel girder and its stiffening plates are assumed to have identical properties as the properties presented in Table 4.3.

The shear connectors were positioned with a number of two in transverse direction. They were located as is illustrated in figure 4.2, with a distance of 62,5 mm from the edges.

Table 4.3 S355 properties

Property	Value	Unit
Elastic modulus [E_d]	210 000	MPa
Poisson's ratio, ν	0,3	-
f_y	355	MPa

4.2.2 Concrete slab

To model the concrete, specific properties of concrete must be specified in Abaqus. Concrete need even further information due to its complexity, which are described more thoroughly in chapter 4.4.2. Table 4.4 presents the properties used in the analyses, which are retrieved from (EN 1992-1-1, 2005).

Table 4.4 Concrete and reinforcement properties

Property	Value	Unit
E_{cm}	35 000	MPa
Poisson's ratio, ν	0,19	-
$f_{c,cyl}$	32	MPa
$f_{c,cu}$	40	MPa
f_{tcm}	2,8	MPa

f_{tcm} is according to (Nilforoush & Shahrokh Esfahani, 2012) calculated by $0,24 * f_{cu}^{\frac{2}{3}}$. The geometry of the concrete slab is rectangular with a height of 150 mm and a width of 1000 mm. The $f_{c,cu}$ value are used in the simulations.

4.2.3 Rebars

(Dassault Systèmes, 2013) recommends the modeling of rebar's in a shell-element by defining rebar layers and using the embedded technique if the concrete-element is solid. Below in table 4.5 are the properties used to define the reinforcement. These properties are taken from (EN 1992-1-1, 2005).

Table 4.5 Reinforcement properties

Reinforcement yielding limit [f_{ry}]	500	MPa
Reinforcement elastic modulus [E_{ra}]	200 000	MPa

Four rebar layers were defined, two rebar layers were considered in the longitudinal direction and two rebar layers in the transverse direction. All the rebar layers have a clear distance of 150 mm between each other and a diameter of 12 mm.

A cover distance of 15 mm is considered between the edge of the concrete slab and the two transverse layers of rebars. Both the layers in longitudinal direction are directly above or below the transverse layer and represents the flexural reinforcement.

4.3 Boundary Conditions and Loading

The composite beam is modeled as simply supported. To achieve this boundary condition the model has one support that is constrained in the x-, y-, and z-directions. The other support is constrained in x- and z-directions. The supports do not limit the rotation in any direction.

The shear connectors are modelled in Abaqus as a so-called Cartesian connector. This kind of connector works in a pre-defined coordinate system and is able to move in x-, y-, and z-directions. The connectors' properties are described in chapter 4.5.

The connection between the steel plates and the steel beam is defined as a "tie connection". The tie connection does not allow any movement of the individual component. This is chosen to represent the welding between the two components and an assumption that there will be no failure at that position is made.

The connections between steel-concrete surfaces is very important in a FEA to get as realistic results as possible. In this case, the interface between the steel beam and concrete slab is defined by means of tangential and normal elements. The friction formulation for the tangential elements is set to penalty, which allows the contact an elastic slip when the force is applied. In addition, a friction coefficient of 0,45 was applied as recommended previously in (Raous & Ali Karray, 2009). For the normal contact elements, a hard contact is chosen as Pressure-overclosure since the steel and concrete at the interface layer do not penetrate to each other. However, separation or uplift can occur for the normal contact elements, which is likely to happen at the ends of the steel girder when slip occurs.

The steel-beam is chosen to be master surface and the concrete slab is selected as slave surface. This is done according to the criteria stated in (Dassault Systèmes, 2013), that the element with a stiffer body and a coarser mesh should be assigned as master surface.

The load case is supposed to represent a point load. To avoid stress concentration around the point of loading, which can result in local crushing of concrete and consequent run time error in Abaqus, a uniform load is applied on an area of 300*300 mm in the middle of the concrete surface. The uniform load is recalculated to represent the same force as a point load would do.

4.4 FE Discretization

The steel beam, steel plates and the concrete slab can be modeled by shell elements or solid elements. In this study they are modeled by shell elements. Shell elements are mainly selected to save the time for analysis as they can reasonably well present the behavior of composite beams.

The steel beam and steel plates are meshed with a technique called "structured". The concrete slab is not possible to mesh with a structured technique due to the uniform load that is applied on top of it. Instead, a technique called "free" has been used for the concrete slab.

A mesh-convergence study is performed to see if the size of mesh elements has any influence of the numerical results and also to choose a realistic mesh size for the elements. The aim of this study is partly to verify the results of the numerical analysis. For this reason, the non-composite steel-concrete beam was simulated at various mesh sizes. The size of mesh elements has been refined until the numerical results converged reasonably. The mesh size varied from 120 mm up to 160 mm. The suitable mesh size which resulted in convergent results was 145 mm for concrete slab and 50 mm for steel

girder. It should be noted that the time of analysis increases by refining the mesh size as the total number of elements increases. This must be considered when performing a mesh-convergence study.

To exclude the influence of size of mesh elements on the numerical results of different FE models, the other FE models for the composite beams with partial and full composite reactions were modeled with the same size of mesh elements as chosen in the non-composite beam. There are 2380 elements in the steel beam, 40 elements in each stiffening steel plate and 368 elements in the concrete slab. In total, the FE models have 2988 mesh-elements. An illustration of the discretized FE model is shown in figure 4.3.

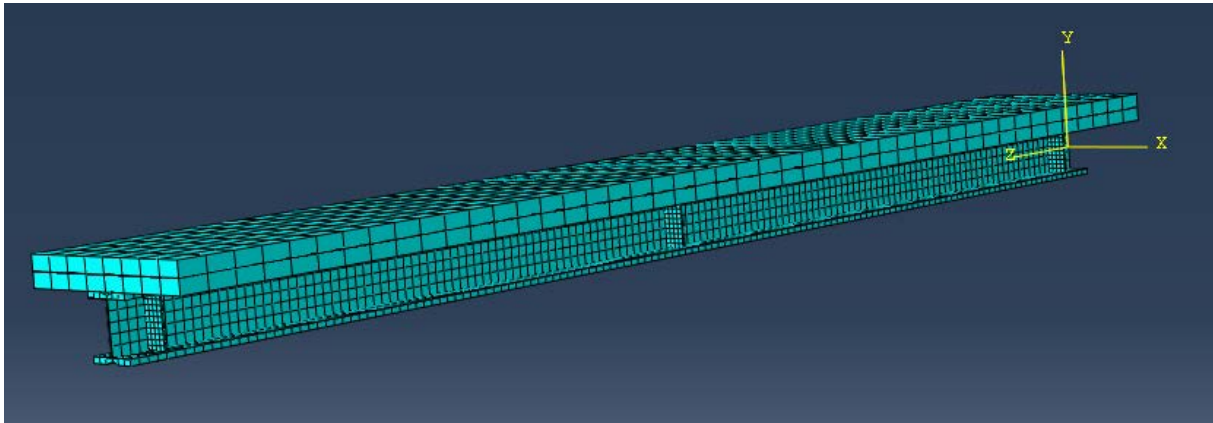


Figure 4.3 The FE-model shown with the mesh visible

4.5 Material Model

In Abaqus, there are a few parameters that must be known to describe the materials that are going to be used. The density, elastic modulus, poisson ratio and a stress-strain curve are required to describe the material needed in this analysis. Concrete needs even more parameters to fulfill a realistic behavior. There are some different methods and formulas that are possible to use to describe a materials behavior and each assumption is described later in this section.

4.5.1 Steel

Steel is an isotropic material, which implies that it has the same properties in compression and tension. In a numerical analysis, the methods can be simplified depending on what result you are expecting. The material model can for an example be simplified as shown in figure 4.4 (a), (b) and (c).

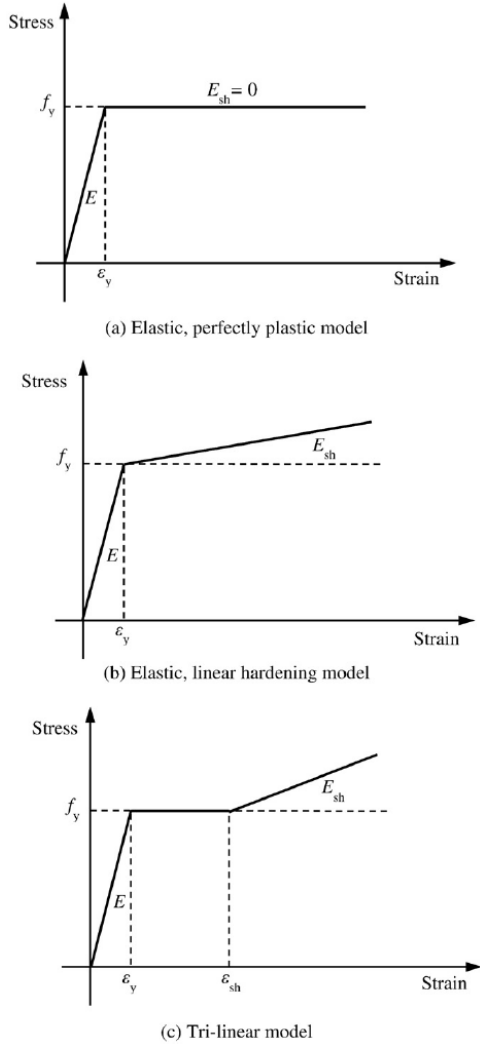


Figure 4.4 Different stress-strain relationships for steel (redrawn from Yun & Gardner, 2017)

Even more advanced stress-strain relationships can be applied to get a more realistic model. The non-linear hardening model proposed by (Yun & Gardner, 2017) is assumed to be linear elastic between zero-strain and the steel yield strain ε_y . The stress in yielding is constant while the strain increase to ε_{sh} . Between ε_{sh} and ε_u , the strain hardening is non-linear and calculated by eq. 4.4. When the stresses are calculated based on different strains, the stress-strain diagram will look as the one in figure 4.5.

$$f(x) = \begin{cases} E\varepsilon, & \varepsilon \leq \varepsilon_y \\ f_y, & \varepsilon_y < \varepsilon \leq \varepsilon_{sh} \\ f_y + (f_u - f_y) \left\{ 0,4 \left(\frac{\varepsilon - \varepsilon_{sh}}{\varepsilon_u - \varepsilon_{sh}} \right) + \frac{2 \left(\frac{\varepsilon - \varepsilon_{sh}}{\varepsilon_u - \varepsilon_{sh}} \right)}{\left[1 + 400 \left(\frac{\varepsilon - \varepsilon_{sh}}{\varepsilon_u - \varepsilon_{sh}} \right)^5 \right]^{\frac{1}{5}}} \right\}, & \varepsilon_{sh} < \varepsilon \leq \varepsilon_u \end{cases} \quad (4.4)$$

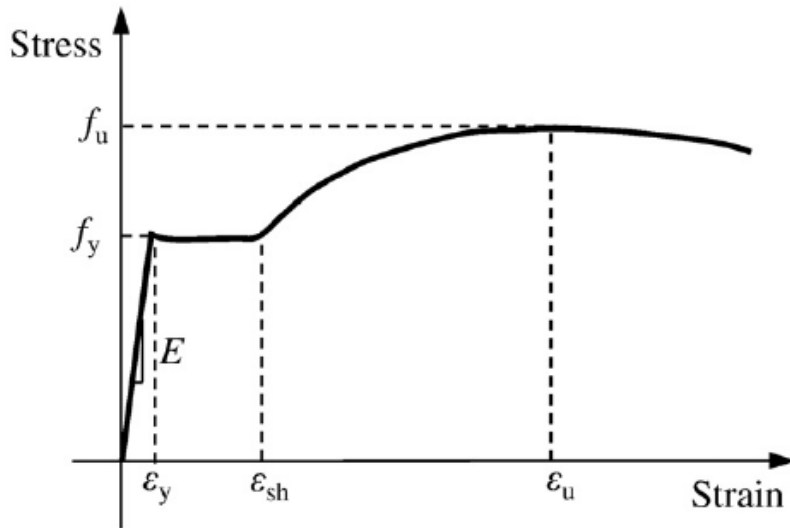


Figure 4.5 A stress-strain diagram of hot-rolled steel

In this analysis the “elastic perfectly-plastic” model shown in figure 4.4(a) is being used to describe the material steel. It is due to there is no need to go any further into the plastic behavior in this analysis. The analysis is finished when the stresses reaches its yielding limit. The material model is used for the steel beam, steel plate and the reinforcement.

4.5.2 Concrete

As concrete is not an isotropic material, the stress-strain curve must be described differently in compression and tension. Since the behavior of concrete is different after cracking, other parameters need to be described. According to (Dassault Systèmes, 2013) there are mainly three different models available in Abaqus that can describe the behavior of concrete. In this FEA, the concrete damage plasticity (CDP) model was used.

Compression:

In compression a stress- strain relationship developed by Carreira and Chu and modified by Hsu and Hsu has been used. Formulas and information have been summarized and presented by (Mertol, 2006). An assumption of linear-elastic behavior up to $0.4\sigma_{cu}$ is made according to (EN 1994-2, 2005) and then a non-linear curve based on the equation 4.5 is used. An illustration of the compressive stress-strain relationship can be seen in figure 4.6. The strain must be calculated iterative when the stress is $0,3\sigma_{cu}$.

The relationship used, need conversation to the unit “psi” from MPa to be able to work. A conversion factor of 0,145037743 was therefore used.

In the CDP-model an inelastic strain and not the total strain is given as a parameter. The inelastic strain is the strain after the elastic strain have been subtracted, this can be calculated from eq. 4.6 and 4.7 and is illustrated in figure 4.8.

$$\frac{f_c}{f_c'} = \frac{n\beta\left(\frac{\epsilon}{\epsilon_0}\right)}{n\beta-1+\left(\frac{\epsilon}{\epsilon_0}\right)^{n\beta}} \text{ for } 0 \leq \epsilon \leq \epsilon_{max} \quad (4.5)$$

$$\epsilon_c^{in} = \epsilon_c - \epsilon_{0c}^{el} \quad (4.6)$$

$$\text{Where, } \epsilon_{0c}^{el} = \frac{\sigma}{E} \quad (4.7)$$

β is a parameter who is dependent on the shape of the diagram and is decided by using eq. 4.8 (Mertol, 2006)

$$\beta = \left(\frac{f'_c(\text{psi})}{9460} \right)^3 + 2,59 \quad (4.8)$$

The variable “n” is equal to 1 as $0 \leq \varepsilon \leq \varepsilon_0$ and “n” is also equal 1 when $\varepsilon_0 \leq \varepsilon \leq \varepsilon_{max}$ because f'_c is less than 62 MPa (Mertol, 2006).

ε_0 and E_{it} are calculated throw eq. 4.9 and eq. 4.10 and they are both obtained by a regression analysis (Mertol, 2006).

$$\varepsilon_0 = 8,9 * 10^{-8} f'_c(\text{psi}) + 2,114 * 10^{-3} \quad (4.9)$$

$$E_{it} = 1,2431 * 10^{-1} f'_c(\text{psi}) + 3,28312 * 10^3 \quad (4.10)$$

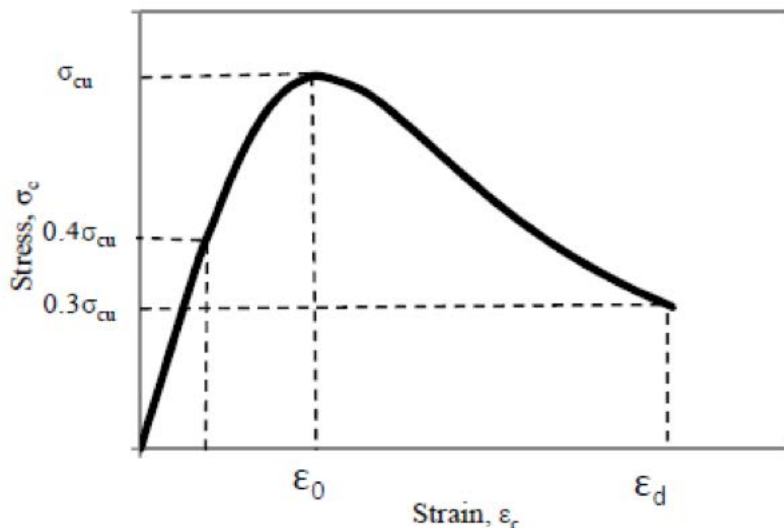


Figure 4.6 Compressive stress-strain diagram, redrawn from (Wahalathantri, Thambiratnam, Chan, & Fawzia, 2011)

Tension:

The stress-strain model first tested in the analysis is presented by Nayal and Rasheed’s and modified by (Wahalathantri, Thambiratnam, Chan, & Fawzia, 2011) to avoid errors in the numerical analysis. The

model is assumed to be linear-elastic to σ_{t0} and then have linear-plastic behavior after the peak stress as in figure 4.6.

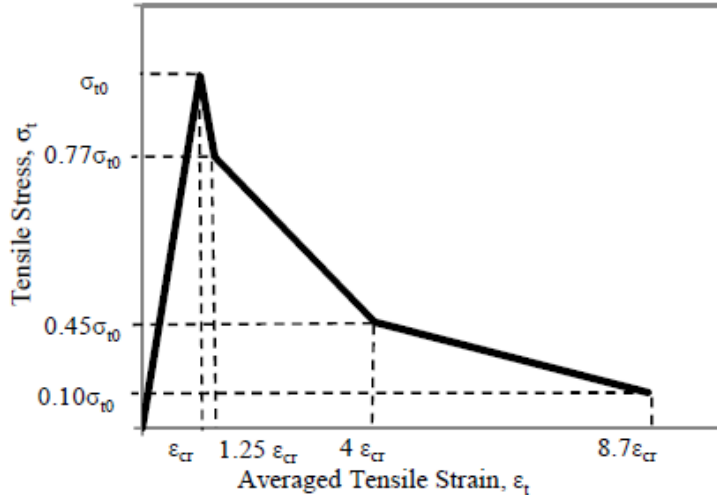


Figure 4.7 Modified tensile Stress-strain diagram (Wahalathantri, Thambiratnam, Chan, & Fawzia, 2011)

When using the stress strain curve presented by (Wahalathantri, Thambiratnam, Chan, & Fawzia, 2011) the analysis gave run time error and were not able to complete. Instead a tension stress-strain curve obtained from (Jankowiak & Łodygowski, 2005) were used. This is a simplification done due to their tension model has almost the same f_{ctm} as calculated in this thesis. The values used in tension to describe the stress-strain relationship are presented in Appendix B.

Damage factor:

The CDP model is based on taking a damage factor into account to degrade the stiffness in the concrete. This is shown in Figure 4.8 and are being done as the stress has reached its peak and the stress is descending (Birtel & Mark, 2006). To calculate the damage factors in tension and compression, formulas described by (Birtel & Mark, 2006) is used and shown in Eq. 4.11 and 4.12

$$d_c = 1 - \frac{\sigma_c * E_c^{-1}}{\varepsilon_c^{pl} \left(\frac{1}{b_c} - 1 \right) + \sigma_c * E_c^{-1}} \quad (4.11)$$

$$d_t = 1 - \frac{\sigma_t * E_c^{-1}}{\varepsilon_t^{pl} \left(\frac{1}{b_t} - 1 \right) + \sigma_t * E_c^{-1}} \quad (4.12)$$

Where $b_c = 0,7$ and $b_t = 0,1$, based on experimental data of cyclic tests. (Birtel & Mark, 2006)

The plastic strain corresponding to inelastic strain must be calculated to find the damage parameter. These equations are shown in eq. 4.13 and 4.14.

$$\varepsilon_c^{pl} = b_c * \varepsilon_c^{in} \quad (4.13)$$

$$\varepsilon_t^{pl} = b_t * \varepsilon_t^{in} \quad (4.14)$$

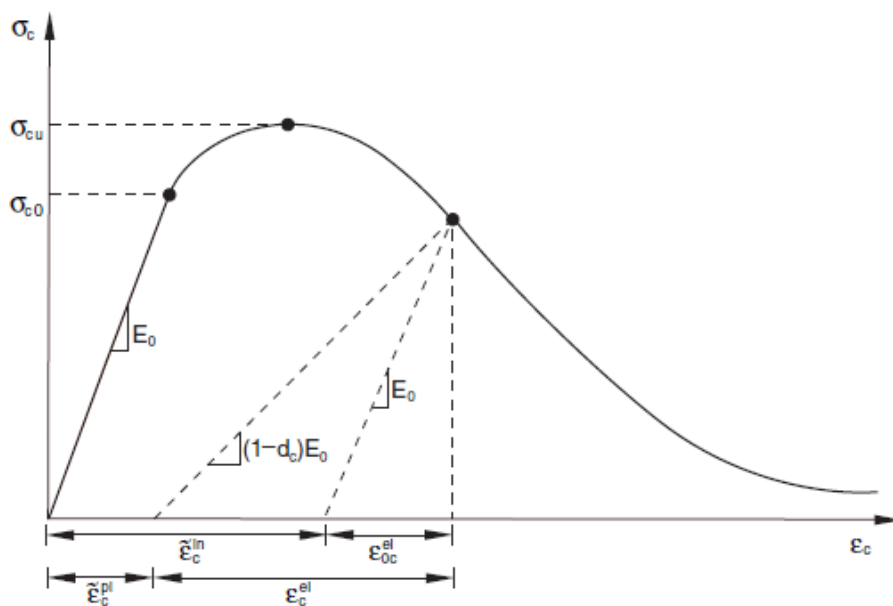


Figure 4.8 Stress-strain diagram in compression affected by damage parameter, redrawn from (Dassault Systèmes, 2013)

Other parameters used in CDP:

To define the yield surface in concrete, five parameters has to be defined. In this case the parameters recommended by the research of (Jankowiak & Łodygowski, 2005) are used and shown in table 4.6. Abaqus standard parameters are being presented in table 4.7 as comparison. The viscosity has been chosen to 0,003 to achieve less restriction at the analyses. To get an even more realistic behavior, laboratory experiments to receive these parameters are necessary.

Table 4.6 CDP parameters obtained by (Jankowiak & Łodygowski, 2005)

Parameter	Value
Dilation angle	38
Eccentricity	1
f_{b0}/f_{c0}	1,12
k	0,666
Viscosity	0,003

Abaqus has its own standard values that would probably give good result as well. Abaqus standard parameters are pretty close to the values presented by (Jankowiak & Łodygowski, 2005), which can be seen in table 4.7.

Table 4.7 Abaqus standard parameters in a CDP model

Parameter	Value
Dilation angle	36
Eccentricity	0,1
f_{b0}/f_{c0}	1,16
k	0,666
Viscosity	0

4.6 Shear Connector

The shear connectors were modeled as a non-linear connector element with properties achieved by push out tests, obtained by (Hällmark, Collin, & Hicks, 2018b). In Abaqus, the user defines at which force the connector allows a specific displacement. The data used to describe the CSP's behavior in these analyses is shown in figure 4.10.

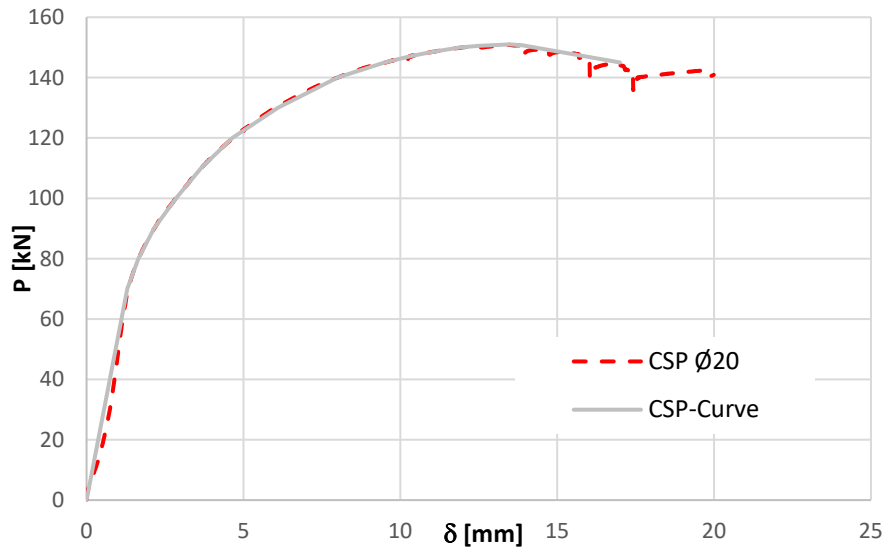


Figure 4.9 Force - displacement relationship of a CSP

A connector type called Cartesian is chosen based on the ability to move along a pre-defined coordinate system. The CSP's are connected through the bottom of the upper flange to the middle of the concrete slab and have a physical diameter of 20mm. An illustration of a typical connector in Abaqus is shown in figure 4.10.

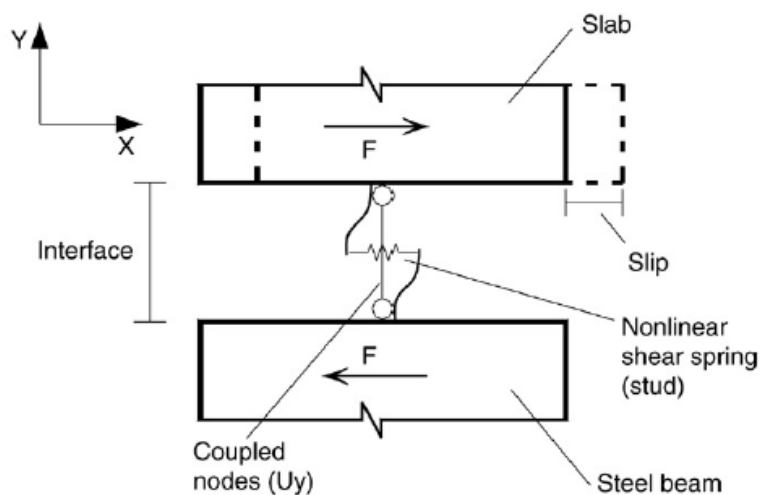


Figure 4.10 Illustration of a connector in a FEA, redrawn from (Dassault Systèmes, 2013)

4.7 Implementation of Analyses

To decide the maximal load before failure and to be able to calculate how many CSP's per meter that are necessary to achieve full-composite action, a test analysis with 10 CSP's/m is performed and the

result showed that maximal load before yielding in the bottom flange is 588kN. Hand calculations according to (EN 1994-2, 2005) is then performed with the failure load obtained numerically to find how many shear connectors is necessarily. The hand calculations can be found in Appendix A.4.

The results of the hand calculations show that 8 CSP's/m are enough to achieve a full-composite action. The span of the girder is 6.6 m and therefore a total number of 54 CSP's are being used. For studying the influence of partial-composite action, two cases were considered in which composite beams with a total of 20 CSP's and 40 CSP's were simulated, respectively. In case 1 and 2, the number of applied CSP's is respectively about 33% and 67% of the case of the full-composite action.

In all cases, it was found that the bottom steel flange reaches its yield strength before the concrete slab fails. The failure load was considered as the maximum load obtained from analysis rounded to the closest integer.

5 Verification of FE Models

To be able to verify the result of an analysis, some sort of verification needs to be done. In this study, the numerical results were compared with the theoretical results obtained from the hand calculations. The stresses in the upper and lower flanges of the steel beam and the deflection at the mid-span are numerically measured. The hand calculations are performed according to (EN 1994-2, 2005). This verification is done to confirm that the material behavior of the steel and concrete is working together as one unit and also working at their own.

5.1 FE verification examples

Two different FE models have been created to verify the reliability in the analysis. A non-linear model with and without composite action is modelled and analyzed.

The model without composite action has no connectors in the structure. The friction factor at the contact between the steel- and concrete surface is 0,45 which gives a more realistic behavior than reducing the friction due to non-composite. This model is later used to find the maximal load which is then compared against all the other beam analyses with CSP's.

The model with composite action has 54 Cartesian connectors applied in two rows as can be seen in figure 5.1, which fully connects the concrete slab with the steel beam. The connectors have an even cc-distance between each other and are fully rigid and are not allowed to move in any direction. The fully rigid connectors will give a more accurate full-composite action than if they were defined to have any deflection, this analysis is and therefore easier to verify.

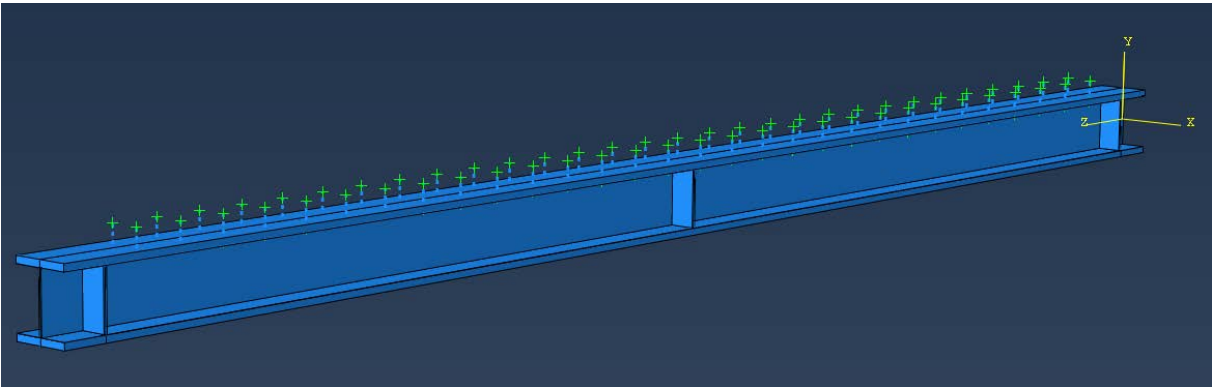


Figure 5.1 Visualization of the full-composite action model with the concrete slab hidden

The applied load in the middle is defined as 4,44MPa, which corresponds to a point load of 400kN. The results from the analysis is shown below in table 5.1.

Table 5.1 FEM calculated stresses and deflection

Stresses/displacement	Non- composite	Full- composite
$\sigma_{top,uf}$ [MPa]	-342	-31
$\sigma_{bottom,lf}$ [MPa]	346	205
u_{middle} [mm]	39	13

5.2 Hand Calculations

Firstly, the cross-section of the steel beam needs to be checked. If the flanges or the web is located in class 4, a reduction has to be performed. After the class for both the flanges and the web are confirmed

to be in class 1 according to calculations in Appendix A.1, calculations of the stresses and deflection can be performed without any reduction. The calculations were performed according to (EN 1994-2, 2005) and can be followed in Appendix A.

The point load is 400kN in the hand calculation and the results are presented in table 5.2.

Table 5.2 Hand calculated stresses and deflection

Stresses/displacement	Non- composite	Full- composite
$\sigma_{top,uf}$ [MPa]	-329	-15
$\sigma_{bottom,lf}$ [MPa]	329	209
u_{middle} [mm]	37	13

5.3 Comparison of FEM and Hand Calculations

To verify the result, a good assumption is that the result of the FEA should approximately be within 10 % of the hand calculations. 10 % is a good guideline and if the difference is larger, the in-data should probably be looked closer into. In chapter 5.3.1 and 5.3.2 the results of the two different analyze cases are compared with hand calculations.

5.3.1 Non- Composite Action

The non-composite girder shows good similarities when comparing the results presented in table 5.3. Both the upper and lower flange shows a difference of about 4-5%. The deflection in the middle is a little higher with 5,4% but represents only 2mm. The result of the comparison shows that the FE-model gives between 4-5,4% higher values compared to the theoretical calculated result.

Table 5.3 Comparison between the results of the non- composite beam

	$\sigma_{top,uf}$ [MPa]	$\sigma_{bottom,lf}$ [MPa]	u_{middle} [mm]
Hand calculations	-329	329	37
FEM	-342	346	39
Difference [%]	4,0	5,2	5,4

Figure 5.2 presents the neutral line where compression stresses transitions to the tension stresses along the non-composite beam. According to theory presented in chapter 2.1, the intersection should be exactly in the middle of the steel beam. As can be seen, this line is located almost in the mid-height of the steel girder which is in very good agreement with the theory. The green line in figure 5.2 and 5.3 illustrates the theoretical neutral axis in the beam.

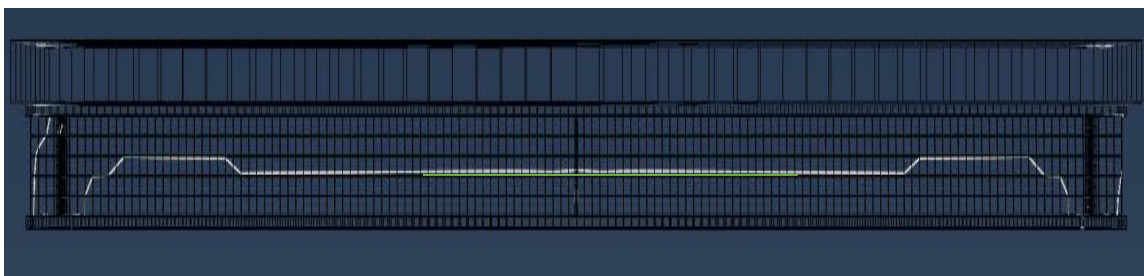


Figure 5.2 The neutral axis of the non-composite beam obtained from FE analysis

5.3.2 Full- Composite Action

The comparison of the numerical results obtained for the beam with full-composite action with the hand calculations according to (EN 1994-2, 2005) indicates that the shear connectors are simulated realistically. However, there is some slip between the concrete and steel representing a partial-composite action rather than a full-composite action.

Table 5.4 Comparison between the results of the full- composite beam

	$\sigma_{top,uf}$ [MPa]	$\sigma_{bottom,lf}$ [MPa]	u_{middle} [mm]
Hand calculations	-15	209	13
FEM	-31	205	13
Difference [%]	106,7	-2,0	0

The comparison shows that in the upper flange, the stress is 16 MPa higher in the analysis. This result is much larger than the hand calculations and describes that there is a small slip between the steel beam and the concrete slab, which is not 100% full-composite action as the theoretical.

Just as in figure 5.2, the line between compression and tension stresses is shown in figure 5.3 and 5.4. According calculation made by eq. A.18 in appendix A, the intersection should be 21 mm below the top of the upper flange when there is full-composite. In figure 5.3, the line cannot fully be seen due to the line is above the flange somewhere in the upper flange, just as calculated.

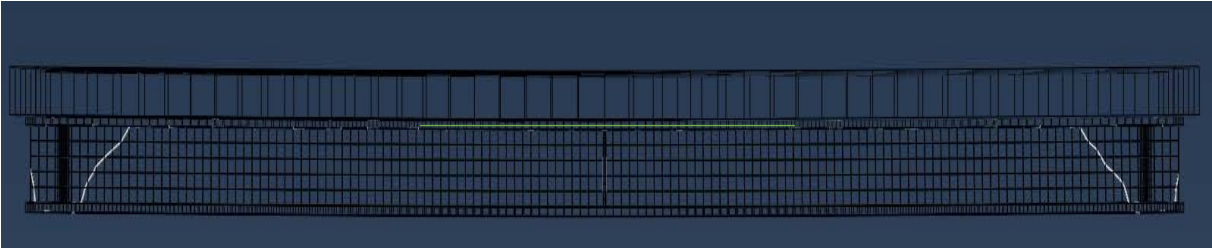


Figure 5.3 The neutral axis of the full-composite beam with rigid shear connectors obtained from FE analysis

In figure 5.4 where 54 coiled spring pins has been analyzed, the line is somewhere between the upper flange and the middle of the flange. This indicates that a partial-composite action is achieved.

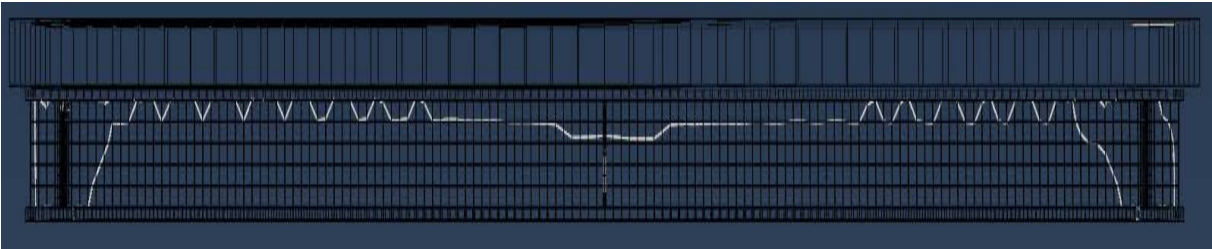


Figure 5.4 The neutral axis of the full-composite beam with CSP shear connectors obtained from FE analysis

6 Numerical Studies

As mentioned in the first chapter, the main goal of the FE-analysis was to compare the maximum load of the non-composite beam with the maximum load of full composite beam, before the lower flange starts to yield or the concrete slab crushes. The result of maximum load before failure is presented in chapter 6.1.

Two different cases will be analyzed to see if the location of the CSP's are of a major importance as suggested by (Kwon G. , 2008). Case 1 will focus on a composite beam with connectors placed locally close to the supports and case 2 is focusing on a composite beam with the same number of connectors which are evenly distributed along the girder.

Also, a partial-composite action is designed when the number of CSP's is less than the designed number for achieving full-composite action, which is done below in chapter 6.4. Where it will be analyses of different numbers of CSP's per meter to find out whether a partial composite action is effective as much as a full composite action.

The analyses that has been performed is shown in table 6.1. The different number of CSP's is performed to see the structural behavior of a non-composite beam that are strengthened with Coiled Spring Pins. It is also shown in these analyses if a partial composite action is as effective as with a full composite action. With the results from case 1 and case 2, the importance of the placement with CSP's can be concluded. In chapter 6.1.1 the influence of fully-rigid connectors and non-linear shear connectors with CSP properties are compared.

Table 6.1 Performed analyses

Performed analyses	Positioning of CSP's	Total number of CSP's
Different number of CSP's	Evenly distributed	0, 8, 14, 20, 28, 34, 40, 48, 54, 60, 66 & 74
Case 1	Centered to the supports	20 & 40
Case 2	Evenly distributed	20 & 40
Uplift & Slip	Evenly distributed	0, 20, 40 & 54

To make the visualization of the connectors placing easier, the concrete slab is hidden in figure 6.1 and 6.3 below, just as in figure 5.2.

6.1 With and Without Full-Composite Action

To analyze full-composite action with CSP's installed, the model looks exactly like figure 5.2 where the fully rigid connectors were applied. But this time the CSP-data presented in figure 4.9 is used. The maximal load is found out to be 580kN before the lower steel flange reaches its yielding limit.

When the model has no composite action, the load applied before the lower steel flange starts to yield is 409kN. With hand calculations performed a theoretical load of 431kN should be possible. This shows a value of about 5% lower than theoretical.

The increases of load are significant larger when CSP's are added, and composite-action is obviously achieved. According to hand calculations the perfectly full-composite action before yielding is 679kN.

It is a big difference between the coiled spring pins maximal load and the fully-rigid shear connectors. The fully rigid connectors allow no displacement and are therefore resulting in a higher degree of composite action.

6.2 Case 1 (CSP's concentrated near the supports)

In literature as (Kwon G. , 2008) it is stated that concentrating the shear connectors closer to the support could give a higher composite effect than an evenly distributed placed shear connector when applying partial-composite action. To test this with CSP-connectors, 37% and 74% of the total amount is put closer to the support. This is done with a c-c distance of 200 mm between the connectors and the first row is 200 mm away from the support. An illustration of this with 20 shear connectors is shown in figure 6.1.

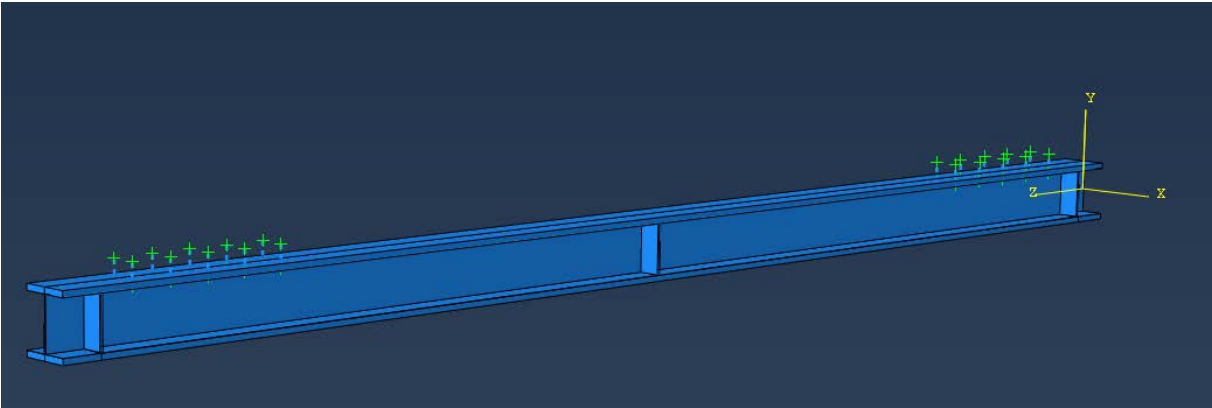


Figure 6.1 20 CSP's concentrated close to the supports

In Figure 6.2, the partial-composite action increases as the number of shear connector increases. From non-composite action to a partial-composite ratio of 37%, the increase in maximal load is 24,0%. And from zero composite to 74%, the increment is 35,7%

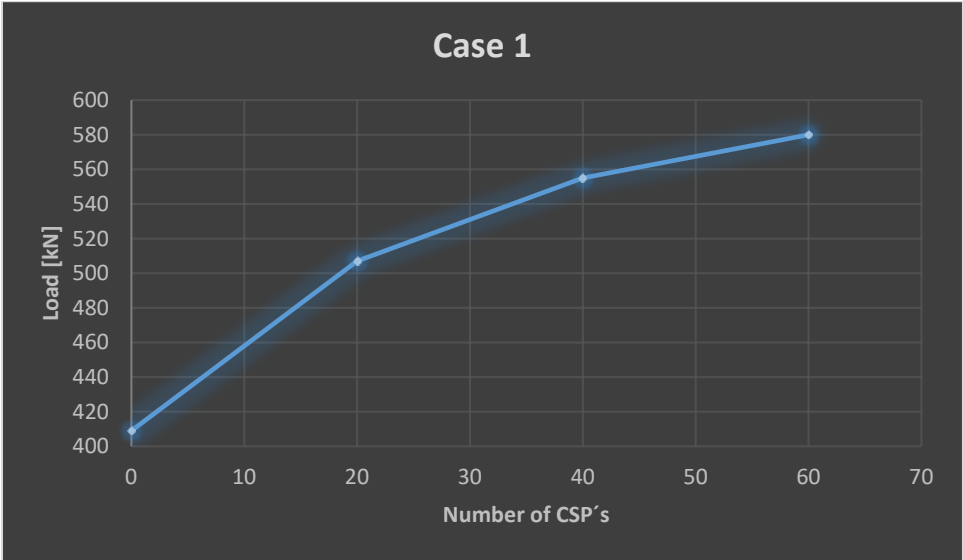


Figure 6.2 Results from case 1

6.3 Case 2 (evenly distributed CSPs)

The other case tested is evenly distributed CSPs along the beam longitudinal direction as can be seen in figure 6.3. In this case, a total of 20 and 40 CSP's are placed along the beam in two different models. The CSPs are positioned at a distance of 200 mm from the beam supports and evenly distributed along

the beam at 688,9 mm and 326,3 mm center to center spacing, depending on number shear connectors.

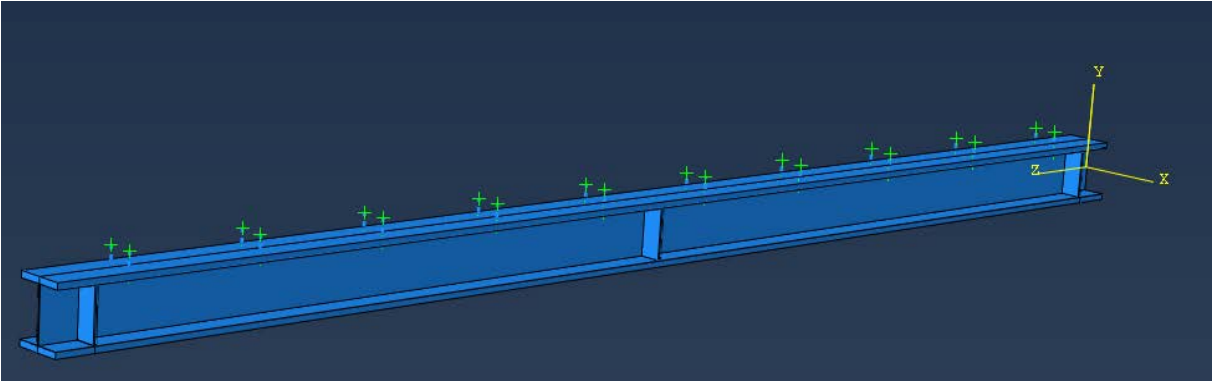


Figure 6.3 The FE model with 20 CSP's evenly distributed

Just as in case 1, a large strengthening is seen in figure 6.4 when coiled spring pins have been installed. When 74% of the total number connectors installed the result is almost the same as case 1, a load of 3kN higher is possible in case 2. With 37% installed the increment of load is 25,2% instead of 24% that is achieved in case 1. It seems that there is no major difference depending on the positioning of the connectors in this case. But evenly distributed shear connectors would be favorable in this analysis.

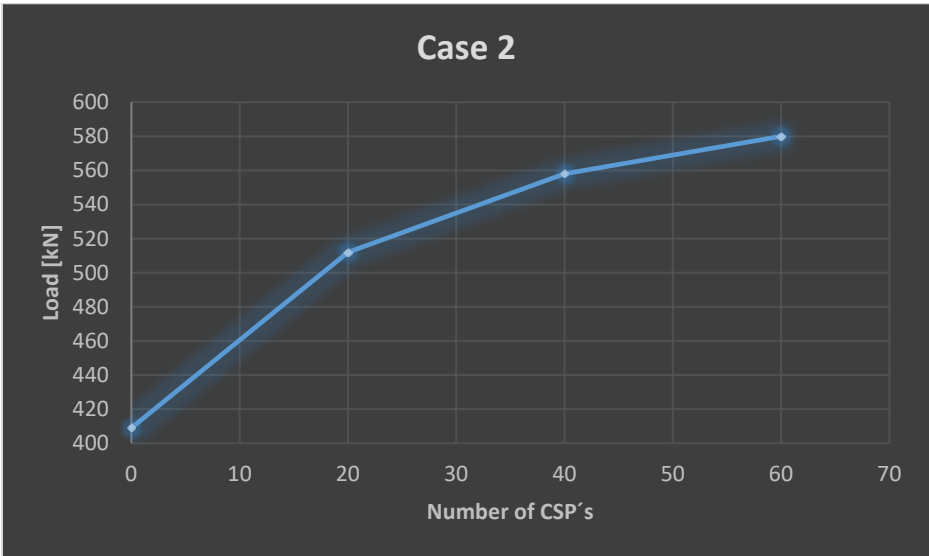


Figure 6.4 Results from case 2

6.4 Different number of CSP's per meter

In this analysis the maximum load before yielding in the lower flange is studied with different number of CSP's per meter. The calculation of the total number of shear connectors is based on the nearest even number upwards. The total length between the supports is 6,6 m and multiplied with CSP/m gives the total number used in the analysis. The first and last row of shear connectors have a distance of 200 mm to the support. Figure 6.5 presents the results of the different maximal loads depending of number CSP's per meter.

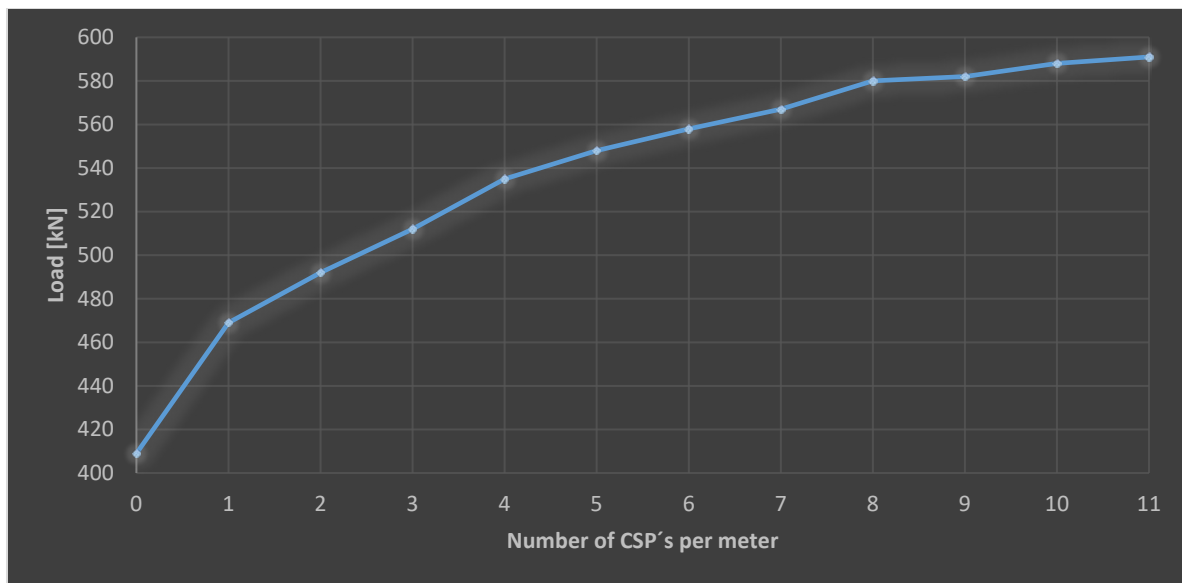


Figure 6.5 Results of different number CSP's per meter

The results presented in table 6.2 includes the percentage of increased load compared to non-composite action as well the shear connection ratio. The maximal load increases even after the full-composite action is achieved due to each connector takes less load and therefore allows a lower displacement.

Table 6.2 Summary of increased load and shear connection ratio with different number of CSP 's per meter

CSP/m	Total No. CSP's	Shear ratio [%]	Maximal load [kN]	Increase compared to non-composite action [%]
0	0	0	409	0
1	8	15	469	14,7
2	14	26	492	20,3
3	20	37	512	25,2
4	28	52	535	30,8
5	34	63	548	34,0
6	40	74	558	36,4
7	48	89	567	38,6
8	54	100	580	41,8
9	60	111	582	42,3
10	66	122	588	43,8
11	74	137	591	44,5

What is noticed in table 6, is that the specimen with two CSP's directly under the load have a slightly higher increase of percentage than the specimen that doesn't have shear connectors directly below the load. For an example, 8 CSP's per meter has an increase of 3.2 percent units when six shear connectors are added compared to 9 CSP's per meter, which only have an increase of 0,5 percent units

when added the same number of connectors. When the amount of shear connectors is increased, the percentage unit are decreasing compared to the previous specimen.

All analyses have ended with the bottom steel flange reaching its yielding state. The concrete did not go to failure and did not reach its highest stress in either compression or tension.

A small parameter study where performed to see the result of using the steel quality S420 instead of S355 in the steel beam and steel plates. The result showed that without composite action, failure occurred in the lower steel flange at a load of 477kN. When 54 coiled spring pins where installed and full-composite action is achieved, the load increased to 681kN. This is an increase of the maximal load by 42,8%. Comparing this increase to the quality of S355, the percentage is almost the same. 1 percentage unit higher is achieved by using a higher steel quality in this analysis.

6.5 Slip and Uplift

Slip is the difference in the horizontal displacement of the respective nodes on the top flange and concrete shell. Uplift is the difference in the vertical displacement. In figure 6.6, the data calculated by Abaqus is visualized when a load of 400 kN was applied at the non-composite girder. The nodes of booth elements were at the middle and the end of the girder. In figure 6.6, number “1” is the slip in transverse direction of the girder, number “2” is the uplift and number “3” is the slip in longitudinal direction.

```

Node: STEEL_BEAM-1.12
Base coordinates:      0.00000e+000, 1.25000e+002, 7.00000e+003, Magnitude
Scale:                1.00000e+000, 1.00000e+000, 1.00000e+000, -
Deformed coordinates (unscaled): 1.04136e-003, 1.28200e+002, 6.99580e+003, -
Deformed coordinates (scaled):   1.04136e-003, 1.28200e+002, 6.99580e+003, -
Displacement (unscaled): 1.04136e-003, 3.20040e+000, -4.20137e+000, 5.28148e+000

Node: CONCRETE_SLAB-1.96
Base coordinates:      1.19049e-001, 2.30000e+002, 7.00000e+003, Magnitude
Scale:                1.00000e+000, 1.00000e+000, 1.00000e+000, -
Deformed coordinates (unscaled): -1.43218e-001, 2.33200e+002, 6.99969e+003, -
Deformed coordinates (scaled):   -1.43218e-001, 2.33200e+002, 6.99969e+003, -
Displacement (unscaled): -2.62267e-001, 3.20015e+000, -3.07220e-001, 3.22554e+000

Nodes for distance: STEEL_BEAM-1.12, CONCRETE_SLAB-1.96
Base distance:        1.19049e-001, 1.05000e+002, 0.00000e+000, Magnitude
Scale:                1.00000e+000, 1.00000e+000, 1.00000e+000, -
Deformed distance (unscaled): -1.44259e-001, 1.05000e+002, 3.89404e+000, 1.05072e+002
Deformed distance (scaled):   -1.44259e-001, 1.05000e+002, 3.89404e+000, 1.05072e+002
Relative displacement (unscaled): -2.63308e-001, -2.43902e-004, 3.89415e+000, 3.90304e+000

```

Figure 6.6 Data of the relative displacement from the analyze of the non-composite girder.

In both table 6.3 and 6.4, it can be seen that the slip decreases as the number of coiled spring pin increases. Even when a load of 580kN at the girder with full-composite action, the slip is much lower than the other cases with lower number of shear ratio. The data of these two tables are therefore showing that the coiled spring pins are reducing the slip a lot compared to a non-composite action girder.

Table 6.3 Slip and Uplift analyzed at a load of 400kN

Number CSP's	Slip [mm]	Uplift [mm]
0 CSP's	3,8942	-0,0002
20 CSP's	1,0189	0,0725
40 CSP's	0,3905	0,0669
54 CSP's	0,2038	0,0663

The uplift seems also to decrease as the number of CSP's increases, but is almost constant when higher load is applied at different shear ratios. At 0 CSP's the uplift has a very small negative displacement, which means that the elements are getting closer to each other.

Table 6.4 Slip and Uplift analyzed at a point load of the maximal load possible at each number of CSP's

Number CSP's	Slip [mm]	Uplift [mm]	Load [kN]
20 CSP's	1,5917	0,1038	512
40 CSP's	0,6597	0,0991	558
54 CSP's	0,3157	0,1004	580

6.5.1 Vertical Displacement

The Vertical displacement is also analyzed at the composite girder. This is done at the midspan of the lower flange in all four conditions, at their maximal load before failure.

Table 6.5 Vertical displacement at midspan of the lower flange

Number CSP's	Vertical displacement [mm]	Load [kN]
0 CSP's	39,1476	400
20 CSP's	31,6355	512
40 CSP's	28,8008	558
54 CSP's	27,9997	580

7 Conclusions

7.1 CSP

After the 54 CSP's have been installed the maximal load before the failure in the lower steel flange occur, increases from 409kN to 580kN. This is a load increment of 41,8% and shows that a significant increase of the bridge flexural bending can be increased with post-installing coiled spring pins.

What can be seen from this analysis is that there is no significant different of maximum load before failure in case 1 compared to case 2. The positioning of the CSP's has no major effect if it is evenly distributed across the beam or is concentrated near the supports. The very ductile behavior of the CSP's may be the cause of this result.

After full-composite action is achieved at 8 CSP's per meter, the parentage unit is only increasing about 1 as more connectors are added and that number is decreasing even further. It is probably not economical to add more connectors if the girder needs even more strengthening. Another method would therefore be recommended.

According to (Kwon, et al., 2007), it may be crucial for the economic viability to post-install shear connectors with a partial-composite action instead of a full-composite action. The results in this thesis show that only 74% of the total number to achieve full-composite action is enough to increase the point load with 36,4% instead of 41,8%. If the total number is reduced even further to 26%, the point load will increase with 20,3% compared to non-composite. This will largely decrease the total cost of the bridge strengthening if a lower amount is enough.

A lower number of CSP's will not result in a failure of the studs themselves, it is still the lower flange of the steel beam that reaches yielding. This type of stiffener allows a high displacement when the load increases which results in a lower degree of partial-composite action. Therefore, the steel beam or concrete slab will be the part that first reaches failure.

7.2 Recommendations to the Laboratory Beam Test

- Evenly distributed or concentrated CSP's close to the support does not affect the maximal load according to these analyses, the placement should not matter.
- One beam designed with full-composite action and one with partial-composite action.
- If the main goal of the test is to let the coiled spring pins go to failure, a higher strength quality of concrete and/or other dimensions of the steel beams cross-section is necessary.

7.3 Further Research

- Instead of using shell-element a model with solid-element would be interesting to compare the results with.
- A full-scale beam test is planned to be performed during the spring 2019. A comparison of the FEM-results from this thesis compared to the upcoming results obtained by the beam tests is of high interest. Also, be able to adjust the material models in the analyze is possible after performed tests, due to possible knowledge about the concrete's and steels strength and its behavior.
- It would be interesting to see further results of a parameter study. Adding material data from the planned full-scale beam then comparing different material thicknesses, widths and span lengths to see how the maximal load varies.

8 References

- Birtel, V., & Mark, P. (2006). Parameterised Finite Element Modelling of RC Beam Shear Failure. *ABAQUS Users' Conference*, (pp. 95-108. Retrived from: https://www.researchgate.net/profile/Abdelrahman_Mabrouk2/post/ABAQUS_Concrete_Damage_Plasticity_parameters/attachment/59d6314179197b807798f0ab/AS%3A365173014581249%401464075439654/download/Birtel.pdf).
- Dassault Systèmes. (2013). *Abaqus 6.13 - Analysis User's Guide*. Providence, RI, USA: Dassault Systèmes.
- El-Lobody, E., & Lam, D. (2003). Finite Element Analysis of Steel-Concrete Composite Girders. *Advances in Structural Engineering*, 6 (4), pp. 267-281. doi: 10.1260/13694330322771655.
- EN 1992-1-1. (2005). *Eurocode 2 - Design of concrete structures - Part 1-1: General rules and rules for buildings*. Brussels, CEN - European Comitee for Standardization.
- EN 1993-1-1. (2005). *Eurocode 3 - Design of steel structures - Part 1-1: General rules and rules for buildings*. Brussels, CEN - European Committee for Standardization.
- EN 1994-2. (2005). *Eurocode 4 - Design of composite steel and concrete structures - Part 2: General rules and rules for bridges*. Brussels, CEN - European Committee for Standardization.
- Hällmark, R. (2018a). *Composite Bridges - Innovative ways of achieving composite action*. (Doctoral thesis, Luleå University of Technology, Luleå). Retrived from: <http://www.diva-portal.org/smash/get/diva2:1249244/FULLTEXT01>.
- Hällmark, R., Collin, P., & Hicks, S. J. (2018b). Post-installed Shear Connectors: Push-out Tests of Coiled Spring Pins vs. Headed Studs. *Unpublished manuscript (Submitted in August 2018)*.
- Jankowiak, T., & Łodygowski, T. (2005). Identification of parameters of concrete damage plasticity constitutive mode. *Foundations of Civil and Environmental Engineering*, 6, 53-69. Retrived from: https://www.researchgate.net/publication/228525599_Identification_of_parameters_of_concrete_damage_plasticity_constitutive_model/download.
- Kwon, G. (2008). *Strenghtening Existing Steel Bridge Girders by the Use of Post-Installed Shear Connectors*. (Doctoral thesis, The University of Texas at Austin, USA). Retrived from: <https://repositories.lib.utexas.edu/bitstream/handle/2152/18079/kwond74300.pdf?sequence=2&isAllowed=y>.
- Kwon, G., Hungerford, B., Kayir, H., Schaap, B., Ju, Y. K., Klingner, R., & Engelhardt, M. (2007). *Strengthening Existing Non-Composite Steel Bridge Girders Using Post-Installed Shear Connectors (FHWA/TX-07/0-4124-1)*. Retrived from: National Academy of Science: <https://trid.trb.org/view/839794>.
- Mertol, H. C. (2006). *Behavior of high-strenght concrete members subjected to combined flexure and axial compression loadings*. (Doctoral thesis, North Carolina State University, Raleigh). Retrived from: https://www.ccee.ncsu.edu/srizkal/wp-content/uploads/sites/7/2016/08/Behavior_of_High-Strength_Concrete_Members_Subjected.pdf.

- Nilforoush, R., & Shahrokh Esfahani, M. (2012). *Numerical Evaluation of Structural Behavior of the Simply Supported FRP-RC Beams*. (Master's thesis, Royal Institute of Technology, Stockholm). Retrieved from: <http://www.diva-portal.org/smash/get/diva2:545613/FULLTEXT01>.
- Olsson, D. (2017). *Achieving Composite Action in Existing Bridges - With post-installed shear connectors*. (Master's thesis, Luleå University of Technology, Luleå). Retrieved from: <http://www.diva-portal.org/smash/get/diva2:1066328/FULLTEXT02>.
- Prakash, A., Anandavalli, N., Madheswaran, C. K., Rajasankar, J., & Lakshmanan, N. (2011). Three Dimensional FE Model of Stud Connected Steel-Concrete Composite Girders Subjected to Monotonic Loading. *International Journal of Mechanics and Applications*, 1(1), pp. 1-11. doi: 10.5923/j.mechanics.20110101.01.
- Raous, M., & Ali Karray, M. (2009). Model coupling friction and adhesion for steel-concrete interfaces. *International Journal of Computer Applications in Technology*, 34 (1), pp. 42-51. Retrieved from: <https://arxiv.org/abs/1003.4597>.
- Tahmasebinia, F., Ranzi, G., & Zona, A. (2012). Beam Tests of Composite Steel-concrete Members: A Three-dimensional Finite Element Model. *International Journal of Steel Structures*, 12 (1), pp. 37-45. doi: 10.1007/s13296-012-1004-3.
- Thevendran, V., Chen, S., Shanmugam, N., & Liew, J. R. (1999). Nonlinear analysis of steel-concrete composite beams curved in plan. *Finite Elements in Analysis and Design*, 32, pp. 125-139. doi: 10.1016/S0168-874X(99)00010-4.
- Wahalathantri, B., Thambiratnam, D., Chan, T., & Fawzia, S. (2011). A material model for flexural crack simulation in reinforced concrete elements using Abaqus. In *Proceedings of the First International Conference on Engineering, Designing and Developing the Built Environment for Sustainable Wellbeing* (pp. 260-264). Brisbane: Queensland University of Technology. Retrieved from: <http://eprints.qut.edu.au/41712/>.
- Yun, X., & Gardner, L. (2017). Stress-strain curves for hot-rolled steels. *Journal of Constructional Steel Research*, 133, 36-46. doi: 10.1016/j.jcsr.2017.01.024.

Appendix A – Hand Calculations

The calculations below are performed according to (EN 1993-1-1, 2005) and (EN 1994-2, 2005).

A.1 Classification of Cross-Section Class

No reduction is needed in the yielding limit at the flanges or the web due to the thickness is less than 40mm.

$$\varepsilon = \sqrt{\frac{235}{355}} = 0,81 \quad (\text{A.1})$$

Flanges:

$$c = \frac{b_f - t_w}{2} = 119\text{mm} \quad (\text{A.2})$$

$$\frac{c}{t_f \cdot \varepsilon} = 4,9 \quad (\text{A.3})$$

As equation A.3 is less than 9, the flanges belong to class 1 and there is no need to reduce the cross-section.

Web:

$$c = h_w = 250\text{mm} \quad (\text{A.4})$$

$$\frac{c}{t_w \cdot \varepsilon} = 25,6 \quad (\text{A.5})$$

Due to equation A.5 is less than 72, the web doesn't either need any reduction of its cross-section.

A.2 Non- Composite Action

$$F = 400\text{kN}$$

$$L = 6600\text{mm}$$

$$M_{max} = \frac{F \cdot L}{4} \quad (\text{A.6})$$

$$CG_{steel} = 155\text{mm} \quad \text{Due to symmetry of flanges.}$$

$$A_s = t_{uf} \cdot w_{uf} + t_{lf} \cdot w_{lf} + h_{web} \cdot w_{web} \quad (\text{A.7})$$

The local coordinate system has origin in the top of the upper flange with positive direction downwards.

$$I_{x,steel} = \frac{w_{web} \cdot h_{web}^3}{12} + h_{web} \cdot w_{web} \cdot \left(t_{uf} + \frac{h_{web}}{2} - CG_{steel} \right)^2 + \frac{w_{uf} \cdot t_{uf}^3}{12} + t_{uf} \cdot w_{uf} \cdot \left(\frac{t_{uf}}{2} - CG_{steel} \right)^2 + \frac{w_{lf} \cdot t_{lf}^3}{12} + w_{lf} \cdot t_{lf} \cdot \left(t_{uf} + h_{web} + \frac{t_{lf}}{2} - CG_{steel} \right)^2 \quad (\text{A.8})$$

$$W_{steel,top,uf} = - \frac{I_{x,steel}}{CG_{steel}} \quad (\text{A.9})$$

$$W_{steel,bottom,lf} = - \frac{I_{x,steel}}{CG_{steel} - h_{web} - t_{uf} - t_{lf}} \quad (\text{A.10})$$

Stresses:

$$\sigma_{steel,top,uf} = \frac{M_{max}}{W_{steel,top,uf}} \quad (A.11)$$

$$\sigma_{steel,bottom,lf} = \frac{M_{max}}{W_{steel,bottom,lf}} \quad (A.12)$$

Deflection:

$$u_{steel,middle} = \frac{F*L^3}{48*E_a*I_{x,steel}} \quad (A.13)$$

A.3 Full- Composite Action

$$F = 400kN$$

$$L = 6600mm$$

$$M_{max} = \frac{F*L}{4} \quad (A.14)$$

The local coordinate system has origin in the top of the upper flange with positive direction downwards.

$$CG_c = -75mm$$

$$n_0 = \frac{E_a}{E_{cm}} = 6,563 \quad (A.15)$$

$$A_c = w_c * h_c \quad (A.16)$$

$$A_{comp} = A_c + \frac{n_0}{A_s} \quad (A.17)$$

$$CG_{comp} = A_s * CG_{steel} + \frac{\frac{A_c * CG_c}{n_0}}{A_{comp}} \quad (A.18)$$

$$I_c = \frac{b_c * h_c^3}{12} \quad (A.19)$$

$$I_{x,comp} = I_{x,steel} + A_s * (CG_{steel} - CG_c)^2 + \frac{I_c}{n_0} + \frac{A_c}{n_0} * (CG_c - CG_{comp})^2 \quad (A.20)$$

$$W_{comp,top,uf} = -\frac{I_{x,comp}}{CG_{comp}} \quad (A.21)$$

$$W_{comp,bottom,lf} = -\frac{I_{x,comp}}{CG_{comp} - h_{web} - t_{uf} - t_{lf}} \quad (A.22)$$

Stresses:

$$\sigma_{comp,top,uf} = \frac{M_{max}}{W_{comp,top,uf}} \quad (A.23)$$

$$\sigma_{comp,bottom,lf} = \frac{M_{max}}{W_{comp,bottom,lf}} \quad (A.24)$$

Deflection:

$$u_{comp,middle} = \frac{F*L^3}{48*E_a*I_{x,comp}} \quad (A.25)$$

A.4 Calculations of number CSP's per meter to achieve full composite action

According to (Hällmark, 2018a) the CSP's have an estimated static strength of 130kN/CSP if the minimum thickness of the steel plate is 20mm and the compressive cylinder strength of the concrete is between 24- to 45MPa. When a safety factor of 1,25 according to (EN 1994-2, 2005) is adapted the designed strength is 104kN/CSP.

$$F_{sf} = \frac{\frac{A_{conc}}{n} * (CG_{comp} - CG_c) * V}{l_{x,comp}} = 777kN/m \quad (A.26)$$

$$\text{Where, } V = \frac{F}{2} = 294kN \quad (A.27)$$

And F = 588kN as described in chapter 4.6.

$$\frac{F_{sf}}{104} = 7,5 \quad (A.28)$$

Rounded upwards, the total number of coiled spring pins per meter is 8.

Appendix B – Parameters used in the concrete model

Compression:

Equations 4.5-4.10 are used to calculate the values in table B.1.

Table B.0.1 Stress and strain values in compression used in the CDP-model

True stress [MPa]	True in-elastic strain	d,c
1,605E+01	0	0
2,246E+01	7,123E-05	0
3,083E+01	2,306E-04	0
4,011E+01	1,365E-03	0
3,046E+01	4,926E-03	4,77E-01
2,056E+01	9,238E-03	6,64E-01
1,223E+01	1,712E-02	8,23E-01

Tension:

The values used in tension is withdrawn from (Jankowiak & Łodygowski, 2005).

Table B.0.2 Stress and strain values in tension used in the CDP-model

True stress [MPa]	True in-elastic strain	d,t
1,999E+00	0	0
2,842E+00	3,333E-05	0
1,870E+00	1,604E-04	4,064E-01
8,627E-01	2,798E-04	6,964E-01
2,263E-01	6,846E-04	9,204E-01
5,658E-02	1,087E-03	9,801E-01